Palaeosols in the Upper Pliocene of the Valdelsa Basin (central Italy): a sequence-stratigraphic perspective

Marco Benvenuti[1, 2]*, Anna Andreetta[1], Stefano Carnicelli[1]

1: Dipartimento di Scienze della Terra, Università di Firenze

2: Istituto di Geoscienze e Georisorse, CNR

Email: ma.benvenuti@unifi.it, anna.aandreetta@unifi.it, stefano.carnicelli@unifi.it

*: corresponding author

Abstract

The present study provides an example of how palaeopedology and facies analysis may be integrated for the interpretation of a cyclothemic succession in the Upper Pliocene (Piacenzian) of the Valdelsa Basin (central Italy). The stacking of facies and intervening bounding surfaces, including palaeosols, outline a hierarchy of elementary (EDS) and composite (CDS) depositional sequences within the three unconformity-bounded stratigraphic units (synthems) S4-S6 which compose the succession. The focus of the study is on synthem S4 and the transition to synthem S5. Synthem S4 records the development of a distal alluvial plain dominated by floodbasin mudstone with subordinated channelized sandstone ($S4_1$), followed by the incision of a fluvial valley aggraded by the cyclical stacking of braided and low sinuosity channelized conglomerate and sandstone ($S4_2$). Synthem S5 includes lower shoreface sandstone and inner shelf mudstone related to a major transgression which affected the study area during the late Piacenzian. Evidence of soil forming processes is well preserved in sub-unit $S4_1$ where five palaeosols (PS4a-e) are stacked within the facies architecture of $EDS1_{c\text{-}d}$. Increasing upward soil development was observed within each EDS, with generally better developed soils in EDS S41d. The unconformable transition from S4 to S5 is marked by a thin veneer of slope deposits bearing pedogenic carbonates reworked from a missed PS4f palaeosol formed during the shaping of the erosional surface separating sub-units $S4_1$ and $S4_2$. The results of this study indicate that: 1) the sedimentary and pedogenic processes recorded in the channelized facies and palaeosols in the floodbasin facies of sub-unit $S4_1$, are coherent with a palaeoenvironmental setting dominated by seasonal climate; 2) the facies-palaeosol architecture of S4 synthem, confirms what described in sequence-stratigraphic models applied to continental successions. The pedo-sedimentary signature of the major sea-level fluctuation recorded in the transition between S4 and S5 synthem differs from these models. In this case a well-developed and

drained palaeosol expected to record the maximum regressive surface shaped during the falling stage of sea-level, is missing. This difference is related to a rapid fall and rise of relative sea level which marked the transition between S4 and S5 synthems.

Keywords: Palaeopedology, Fluvial Facies, Composite Sequences, Piacenzian, Valdelsa Basin

1. Introduction

In the continental stratigraphic record, palaeosols are suitable archives for reconstructing ancient surface processes, palaeo-ecosystems and local- to global-scale palaeoclimate patterns (Kraus, 1999; Retallack, 2001; Tabor and Myers, 2015; Costantini, 2018). From a stratigraphic perspective soil formation, indicative of an equilibrium between erosion and deposition, may outline autocyclic processes, such as those occurring within alluvial plains, where gradients in the type and degree of pedogenesis depend on the random migration of channels (Wright, 1992; Kraus, 1999). Alternatively, in the stratigraphic record, palaeosols punctuate the cyclic creation and destruction of sediment accommodation, due to the interplay of such allogenic forcing factors as eustasy, tectonics and climate (Shanley and McCabe, 1994). With the advent of sequence-stratigraphic models, first established for coastal-marine successions and then applied to continental strata (Wright and Marriott, 1993; Shanley and McCabe, 1994; McCarthy and Plint, 2013; 2014; Raigemborn and Beilinson, 2020), palaeosols have been regarded as specific key bounding surfaces (Fig. 1). In a sequence-stratigraphic perspective, deep, mature and well drained soils record prolonged subaerial exposure of interfluve areas, adjacent to river valleys incised during stages of base/sea level fall. In these terms, palaeosols represent the weathered, non-depositional tract of an erosional unconformity formed within a forced regressive phase. Subsequent variations of base/sea level will cause sediment aggradation within incised valleys, accompanied by changing conditions for soil formation and preservation. During base level lowstands the rate of creation of accommodation is null to low, determining channel amalgamation with little chance for soil preservation. In this stage, soils on interfluve surfaces continue to develop. During transgressive rises of base/sea level, rapid alluvial aggradation determines suitable conditions for the development of poorly-drained, organic-rich soils in muddy plains with isolated ribbon channels. Soils in the interfluves are buried by continuing aggradation. The progression towards the highstand and the related reduction of accommodation is represented in floodplains by both increasing channel amalgamation and more protracted pedogenesis. Renewed fall starts a further depositional cycle with exposure of interfluves and prolonged soil development on stable surfaces.

The present study demonstrates use of integrated palaeosol-facies analyses, aiming at scrutinizing this widely accepted model of soil formation through variation of accommodation space. The case study is offered by an Upper Pliocene (Piacenzian) fluvial succession in Central Italy, characterized by a cyclothemic stack of facies and palaeosols described, in its overall stratigraphic-depositional architecture, in a previous study (Aldinucci et al., 2019).

2. Geological setting

The Valdelsa Basin (Central Italy, Fig. 2A), drained by the Elsa River, is one of the largest late orogenic intermontane basins of the Northern Apennines (Martini and Sagri, 1993; Bonini et al., 2014). Bounded to the southwest by the Mid Tuscan Ridge (MTR) and to the northeast by the Albano-Chianti mounts (ACM), the basin is filled with about 2000 m thick clastic deposits, referred to the late Miocene-early Pleistocene (Ghelardoni et al., 1968). The 1000 m thick, uppermost Messinian-Gelasian, interval is subdivided into the S1 to S7 unconformity-bounded stratigraphic units (Benvenuti and Degli Innocenti, 2001; Benvenuti et al., 2014; Dominici et al., 2018). Synthems S1-S6 formed in response to major relative sea-level fluctuations, typically recorded by lowstand fluvio-deltaic conglomerates and sandstones overlain by transgressive prodelta-inner shelf mudstones, the latter in some cases capped by deltaic and/or alluvial sandstones and conglomerates (highstand deposits, Benvenuti et al., 2014). The uppermost Messinian to Zanclean S1-S3 synthems, characterized by fining- and deepening-upwards facies stacking, are bound by angular unconformities, which attest to a dominant tectonic control on accommodation (Benvenuti et al., 2014; Dominici et al., 2018). The Piacenzian S4-S5 synthems display a composite cyclic facies architecture (Benvenuti et al., 2007; Aldinucci et al., 2019), expressed by the symmetric stacking of regressive and transgressive strata, thus recording a prevailing eustatic signal. The upper Piacenzian to Gelasian S6-S7 synthems form the late infill of the basin and, similarly to S4-S5, display a cyclothemic facies pattern (Benvenuti and Degli Innocenti, 2001; Benvenuti et al., 2007; Aldinucci et al., 2019). The latter, outlining an overall regressive trend from persisting deltaic (S6) to fluvial (S7) facies (Benvenuti et al., 2014), reflects high sediment supply keeping pace or overwhelming the available accommodation. The depositional signature of the S4-S6 synthems has been recently revised following a sequence-stratigraphic approach (Aldinucci et al., 2019). Facies correlation outlined stratigraphic key surfaces, recording relative base/sea-level fluctuations occurred at various time frequencies. The facies architectures bracketed by the different rank regressive (SB1-4, Fig.2D) and transgressive (TS1-3, Fig. 2D) key surfaces allowed to recognize elementary depositional sequences (EDS, Mutti et al., 1994) as the building block of the sequential arrangement. EDS stack into regressive and transgressive sets to define lower rank-composite depositional sequences (Mutti et al., 1994) coinciding with each synthem (CDS1). The stacking of the three CDS1 in turn outlines the regressive and transgressive tracts of a higher-rank composite sequence (CDS2). The available chronostratigraphic constraint for the S4-S6 synthems, as provided by biostratigraphic data (Capezzuoli et al., 2005, Benvenuti et al., 2014), refers the S4 synthem to the mid part of the Piacenzian, including the so-called Mid Piacenzian Warm Period (MPWP, 3.26-3.02 Ma, Dowset et al., 2016). The overlying S5-S6 synthems are calibrated to the upper part of the Piacenzian (Benvenuti et al., 2014). Given the chronological reference of the S4-S6 synthems to the 3.3-2.6 Ma interval, the duration of the EDS, CDS1 and CDS2 is tentatively correlated respectively to the fifth (10^{3-4} years), fourth (10^{4-5} years) and third (10^{5-6} years) order frequencies of the eustatic cycles (Mitchum and Van Wagoner, 1990).

2.1 The study area

The area of the present study (Fig. 2B-C), the Rio degli Apoli catchment, between the Fiano and Marcialla villages (Fig. 2B-C), is located in the SE portion of the basin, about 30 km south-west of Florence (centered at 43°34'34.83"N, 11° 7'10.92"E). Here, the S3 to S7 synthems outcrop (Del Conte, 2007; Benvenuti et al., 2014; Aldinucci et al., 2019). The mud-dominated S3 synthem is generally poorly exposed, whereas the overlying S4-S6 synthems (Fig. 2D) crop out along the steep valley upper slopes; synthem S7, not discussed here, is represented by conglomerates on top of the hills. Specifically, this study focuses on S4 and the transition to S5 synthem. Synthem S4, about 70 meters thick, includes two sub-units, $S4_1$ and $S4_2$ (Fig. 2D), which record a palaeo-drainage directed into coeval coastal settings, southwards (Del Conte, 2007; Benvenuti et al., 2014). Sub-unit $S4_1$ includes EDS $S4_{1a-1d}$, each characterized by the internal transition from lowstand sandy channels (facies S1-S2, table 1) and muddy overbanks (facies P1, table 2) of an alluvial plain to transgressive-highstand mudstones (facies P1, S4) and associated palaeosols, ascribed to a floodbasin. The erosional surfaces SB1 bounding each EDS attest to limited shifts along the depositional gradient as the expression of low-amplitude base-level drops. A single EDS characterizes sub-unit $S4_2$, recording the infill of an incised fluvial valley with amalgamated channel deposits at the base and top (facies CS1, table 1) and an intervening gravelly-sandy laterally-accreted bar (facies CS2, table 1) hinting to a low-sinuosity channel (see Billi et al., 1987; Aldinucci et al., 2019; Fig. 2).

The stacking of facies in S4 is interpreted as a CDS1 formed during a fourth-order cycle of base-level change (Aldinucci et al., 2019). The $S41_{a-d}$ elementary depositional sequences record the transgressive and highstand systems tracts followed by a fall of base-level that forced the fluvial incision of sub-unit $S4_1$. This resulted in the erosional bounding surface SB2 attesting to a higher-amplitude depositional shift which brought coarse-grained fluvial deposits to fill up a valley incised in the sand-mud dominated $S4_1$. Aggradation of laterally mobile channel deposits in the valley occurred in a period of null-slow creation of accommodation (Wright and Marriott, 1993; Shanley and McCabe, 1994). Rising of the base-level determined a single low-sinuosity channel, finally replaced again by laterally-mobile channels attesting to a highstand of base-level.

The transition to synthem S5 is marked by a composite, high relief surface which records the maximum depositional shifts associated with relative sea-level fluctuations. Across this surface the S4 alluvial deposits are unconformably overlain by lower shoreface-inner shelf sandstones (facies PS, table 1) and mudstones (facies P2, table 2), documenting a transgression. This surface then bears a double significance, recording a forced regression with the deep incision of a wide palaeovalley, represented in the study area by its eastern flank, followed by rapid marine transgression and onlap of coastal-shallow marine strata. In sequential terms this surface is thus both a high-rank sequence boundary (SB4) and a transgressive surface (TS3, Aldinucci et al., 2019).

Analysis of facies (table 1) and palaeosols (table 2) stacked in the vertical and lateral development of the EDS $S4_{1c-1d}$ and of the unconformable transition between synthems S4-S5 (Fig. 3), was performed in this study and the following sections summarize the results.

3. Materials and methods

3.1 Field observations

Data collection was carried out by integrating standard facies analysis, summarized in table 1, with palaeosol description and sampling on the outcrops. With respect to a previous study (Aldinucci et al., 2019), an extended data collection on the upper portion of $S4_1$ and across the transition to S5 synthem prompted a refined interpretation of the facies-palaeosols relationships within the previously established high-resolution sequence stratigraphic framework.

Palaeosol morphological features observed in the field such as soil structure, Munsell colors and carbonate pedofeatures, were used for the sequence-stratigraphic interpretation. Palaeosols were classified according to the World Reference Bases WRB (IUSS Working Group, 2015), with the necessary adaptations for buried soils. To qualitatively evaluate soil development, we considered the times needed to attain various properties and orders of soils as was presented by Retallack et al. (2001) and Birkeland (1999).

3.2 Stable isotope analyses

Carbon and oxygen isotopes analysis were performed on carbonate nodules collected at different outcrops, to verify their pedogenic origin and as a proxy for palaeoenvironmental conditions. They were then finely ground by hand with an agate mortar and pestle. Samples were analyzed at the Instituto Andaluz de Ciencias de la Tierra (CSIC-UGR). About 5 mg of carbonate powder was placed in a 12ml Exetainer™ vial that was subsequently flushed with helium. The carbonate was converted to CO_2 gas by adding 0.1 ml of 100% H_3PO_4 at 25 °C (McCrea, 1950). Acid fractionation factors used were 1.01044 at 25°C for the calcite (Kim and O´Neil, 1997). The resulting CO_2 was analyzed after 24 h using the GasBench II connected to the Finnigan DeltaPLUS XP isotope ratio mass spectrometer (IRMS). The experimental error for carbonates ($\delta^{13}C$ and $\delta^{18}O$) was ±0.1‰, using Carrara and EEZ-1 as internal standards that were previously compared to NBS-18 and NBS-19. Stable isotope results are reported in δ notation relative to the Vienna international standard Pee Dee Belemnite (V-PDB). The δ values are defined as:

$$\delta^{13}C \ or \ \delta^{18}O = \left[\left(\frac{R_{sample}}{R_{standard}}\right) - 1\right] \times 1000(‰)$$

3. Results

3.1 Facies Analysis

3.1.1 The Elementary Depositional Sequence $S4_{1c}$

The facies stacking within EDS $S4_{1c}$ includes three associated alluvial plain facies (Figs. 3, 4). The basal strata are made of the alternation of facies S1 and P1 (table 1). Facies S1 records the infill of small and narrow ribbon-like channels by vertical aggradation and migration of 3D-dunes from sand-laden flood flows. The shape of trough-cross lamination hints to low-relief sinuous-crested dunes developing under combined conditions of high sediment concentration and fast-flowing tractional currents. In these terms such dunes may represent non-equilibrium bedforms hinting to transition between lower- and upper flow regimes in sediment-laden flows (see Jopling, 1965; Chakraborty and Bose, 1992).

Facies P1 is referred to subaerial sediment settling from mud-bearing flows, successively modified by pedogenic processes. This facies becomes predominant upwards, showing pedogenic features which hint to progressively more marked soil formation (see the palaeosol section). Facies S4, interbedded with P1 (Figs. 3, 4), is referred to varied massive settling and current traction in critical-subcritical regime.

3.*1.2 The Elementary Depositional Sequence $S4_{1d}$*

The uppermost EDS within $S4_1$ sub-unit is mainly represented by facies S2, with intervening strata of facies P1 (Figs. 3, 4). Facies S2 is interpreted as the infill of broad and shallow low-sinuosity channels by laterally-accreted low-relief barforms and migration of 3D-dunes. Facies P1, though subordinate to S4, bears the evidence of the most frequent, well expressed, soil-forming episodes recorded within S4.

3.*1.3 The deposits bracketed within the SB4-TS3 composite surface*

The composite bounding surface separating S4 from S5 synthems includes a few meters-thick succession which was observed in detail along a correlated transect from log 1 to log 2 (Figs. 3, 5, 6). At log 1, SB4/TS3 surface is at its lowest elevation and the bracketed deposit is a 2-meter-thick massive sandy mudstone with floating mm-cm size carbonate nodules (Fig. 5). At log 2 (Fig. 6A) the same composite surface stands at a higher elevation and a bracketed sequence of four graded beds is observed (Fig 6B); these are made of massive silty sandstones with base lags mainly made of carbonate nodules.

3.2 Palaeosol description

3.2.1 The $S4_1$ palaeosols

Different types of palaeosols were observed in sub-unit $S4_1$, across EDS $S4_{1c\text{-}d}$ (Table 2; Fig. 3). A common feature of all such palaeosols is that the solum horizons (A and B) are clay textured, while the underlying (2C or 2Cr) horizons are more silty. All palaeosols have a dark-colored A horizon (Fig. 7A). In PS4a soil, such A horizon lies on a 2Cr horizon; poor horizon differentiation (i.e., the A–C profile) and evident bedding lead to classify palaeosol PS4a as a Fluvisol. PS4b soil could not be formally described, being barely accessible on a sub-vertical cliff. It was anyway possible to verify that it exhibits a Bw horizon which can be defined as a Cambic horizon. Other pedogenic characters, such as secondary carbonates and slickensides, are too poorly expressed to be diagnostic. PS4c soil shows a well-expressed Bss horizon with intersecting slickensides, cracks (Fig. 7B) and common secondary carbonate pedofeatures.

Palaeosols within EDS $S4_{1d}$, PS4d-e (Table 2; Fig. 7C), show pedogenic features similar to PS4c soil. The structure of the Bss horizon is prismatic and moderately developed in PS4d, while it is wedge-shaped, with intersecting slickensides, in PS4e. Carbonate nodules, from a few mm to 2 cm in diameter, show a pattern of increasing size downwards through each palaeosol; they are frequent enough to define a Calcic horizon only in the 2Ck horizon of PS4d, while they are common throughout the Bssk and 2Ck horizons of PS4e. Such nodules define Calcic horizons of Stage II, according to Gile et al. (1966) and Machette (1985). In PS4d soil, the C horizon displays redoximorphic features, including grey/green colors and strong brown oximorphic features, such as coatings around peds, root traces and channels (rusty channels), arranged in a gleyic color pattern (WRB-IUSS Working Group, 2015). In PS4e medium irregularly shaped mottles are common in the 2Ck horizon.

3.2.2. Palaeopedological features of the S4-S5 transition

The thin deposits bracketed by the SB4-ST3 surfaces bear pedogenic features having significant implications for the relationship between soil-forming processes and cyclical deposition. At log 2 (Fig. 6) hard carbonate nodules, ranging from ca. 1 to 4 cm in size, are concentrated at the base of the four stacked beds, and their shape suggests a pedogenic origin (Fig. 7G). Fe-Mn coatings on concretions are abundant in the top bed (Fig. 7F and 7G), then they decrease downwards, to disappear in the basal bed. A well expressed, gleyic-like color pattern with olive (5Y 5/3) matrix color and abundant, yellowish brown (10YR 5/8) oximorphic mottles along cracks and coatings on ped faces, typifies these sediments. At log 1 (Fig. 5), the abundant carbonate nodules, similar in shape and dimension to those seen in log 2, randomly dispersed in the sediment bracketed by the SB4/TS3 surfaces (Fig. 7D and 7E). The pedogenic origin of all these carbonate nodules is confirmed by their isotope composition, with $\delta^{13}C$ and $\delta^{18}O$ values ranging from -11.2 to -8.1‰ and from -5.5 to -4.1‰, respectively (Fig 8).

4. Discussion; palaeosols in the sedimentary record and their implications

4.1 The depositional dynamics across the S4-S5 transition

The described facies stacking is interpreted in terms of depositional processes and systems as follows.

a) The facies associations recognized in $S4_{1c}$ allow to refer the depositional development initially to an alluvial plain, whose elements were relatively deep channels (S1) and floodplain (P1). The sedimentological features of the channel infills suggest infrequent, impulsive high-magnitude floods, as those occurring under seasonal climate regimes (Plink-Björklund, 2015). This setting records conditions of relatively slow creation of accommodation in the late development of the $S4_1$ alluvial plain, due to a low-stand of base level (Wright and Marriott, 1993). The P1-S4 association suggests the deactivation of channels as a possible effect of rising base level and increase of accommodation. This trend resulted in creation of space for the aggradation of muds, occasionally punctuated by the arrival of sand-laden flows depositing small lobes. This setting is referred to a floodbasin, a specific depositional system attesting to a transgressive-highstand stage in the development of a coastal alluvial plain and accommodating mostly fine-grained sediments delivered by overland flows (Benvenuti and Del Conte, 2014).

b) The facies association in $S4_{1d}$ represents the establishment of a broad and shallow low-sinuosity channel belt with channel amalgamation in its lower portion, indicating a slow creation of accommodation. As to the lower portion of EDS $S4_{1c}$ this association records a low-stand of base level, though with the development of a different alluvial plain in terms of geometry and frequency of channels. In the upper portion, channelized sandstones S2 are separated by facies P1 including palaeosols PS4d and PS4e, representing, on the whole, the transgressive-highstand portion of this EDS.

c) The evidence of a thin sedimentary interval bracketed by surfaces SB4 and TS3, and not reported before, hints to gravitative and fluidal transport along the slopes created by the deep incision of S4 deposits. The graded beds observed in the higher position of this palaeo-slope (log 2) are referred to unconfined sediment-laden fluidal flows in which rapid sediment settling concentrated at the base clasts originating from the Calcic horizon of a non-preserved PS4f soil. The massive bed at log 1, located in the lower position along the palaeo-slope, is referred to deposition from a sandy mudflow incorporating clasts from Calcic horizons of the PS4c-f soils, as they were denudated by the progressive surface incision (see below).

4.2 Soil-forming and depositional processes

4.2.1 Soil-forming processes

Main characters of palaeosols within EDS $S4_1$ are due to clay shrink-swell properties (vertic) and carbonate translocation (calcic). The general trend of variation is of increasing soil development upwards within each EDS, with soils in EDS $S4_{1d}$ being generally better developed. In these soils, smectite clays are likely inherited; then, changes in expression of vertic characters should be due either to minor changes in sediment composition or changes in solum thickness, as slickensides' formation requires some depth of overburden soil. In turn, solum thickness is clearly determined by the thickness of the clayey beds on which these soils formed.

Development of calcic features, and finally Calcic horizons, appears instead as a strictly pedogenic character, that can be interpreted as recording the duration of pedogenesis, then of the sedimentary hiatuses, and possibly giving some indication of the then prevailing environmental conditions. Reference data suggest that the minimum time required for the formation of a Vertisol, in what appear to have been favorable conditions, might be as short as 500 years (Pal et al., 2012). Fully developed Calcic horizons, as found in PS4c and PS4e palaeosols, should instead, have required times of the order of 10^3 to 10^4 years (Machette et al., 1985; Retallack, 2001; Carnicelli and Costantini, 2013).

Soil features and the isotopic proxy converge towards indicating a seasonal rainfall pattern. Soil calcic and vertic features' formation are generally considered as recording seasonality (Mermut et al., 1996; Breecker et al., 2009; Huth et al., 2019); similar conditions are indicated by the stable isotope composition of carbonate nodules (Fig. 8), corresponding to those reported for other Mediterranean areas (Cerling and Quade 1993; Cojan et al., 2013), as also proposed by Cerling (1984). This inference matches the sedimentological features of S1-S2 facies, which point to sediment transport and deposition from highly laden flood flows, recalling the sedimentary dynamics of seasonal fluvial systems (Plink-Björklund, 2015).

4.2.2 Evidence of post-burial soil modifications

In the palaeosols within EDS $S4_{1d}$, prevailing good drainage conditions for soil formation, as recorded by calcic features, contrast with gleyic color patterns, recording waterlogged conditions. This suggests water table intrusion late in soil development (Vepraskas, 1999; Driese and Ober, 2005; Sheldon, 2005; Mack et al., 2010; Fidolini and Andreetta 2013), due either to lesser sea level changes or local water table rises caused by the shifting of channels. A similar superposition of calcic and redoximorphic features is found in the sediments at the SB4/TS3 surface, in their upper slope facies at log 2, where it is definitely associated to flooding of the incised palaeovalley. The isotope signature of the SB4/TS3 concretions, plotted in the cross-diagrams of $\delta^{13}C$ and $\delta^{18}O$ values (Quade and Cerling, 2007) and considering the signature of modern environments Cerling (1984), places their setting in a coastal domain. This conclusion is in full agreement with the reconstruction of the S4-S6 depositional settings, as emerged from previous studies (Aldinucci et al., 2019).

4.2.3 Stratigraphic implications of palaeosols and palaeosol sediments

The close association between palaeosols and clayey sedimentary beds suggests how their appearance marks either phases of decreasing aggradation, starting with a fining upwards trend and ending in a sedimentation hiatus, or episodes of changing floodplain positions due to channel shifting. On the other hand, within a succession which is observable for extended tracts (Figs. 1, 3, 4), these palaeosols do not appear to be correlative with erosion surfaces. The PS4a-e palaeosols then represent pedogenic processes fully consistent with the floodplain/floodbasin dynamics recorded by facies association P1-S4.

The differences in palaeosol solum thickness should then be interpreted as recording the thickness of each clay bed, then its significance in the buildup of the succession. It is then significant that the most developed palaeosols appear to be PS4c and PS4e, both being the uppermost palaeosols observed within EDS $S4_{1c}$ and EDS $S4_{1d}$, respectively.

The sediment veneer at the SB4/TS3 surface is marked by the common presence of carbonate nodules whose shape (Figs. 7E, 7G) and isotopic composition (Fig. 8) both point to a pedogenic origin. We then maintain that these nodules came from erosional reworking of Calcic soil horizon materials, eroded from a non-preserved PS4f soil. The missing PS4f was possibly similar to PS4e, but the amount, size and development of carbonate concretions suggest that it was significantly better developed; it could have correlated with erosional surface SB2, separating $S4_1$ from $S4_2$.

4.3 Palaeopedological implications for a sequence-stratigraphic model

The soil-forming processes in the composite sequential development of the studied succession mostly follow the evolutionary trends predicted in well-established non-marine sequence-stratigraphic models (Wright and Marriott, 1993; Shanley and McCabe, 1994). The stacking of EDS in the late development of sub-unit $S4_1$ coincided with an highstand system tract of the related CS1 (Fig. 3, 9). The overall picture of soil development during the deposition of EDS $S4_{1c-d}$ complements sedimentary facies analysis and allows to further detail sequence stratigraphic reconstructions. Palaeosols within EDS $S4_{1c}$ attest to an aggradation phase punctuated by short-term slowdowns and standstills, these last becoming more significant towards the top. Palaeosols within EDS $S4_{1d}$ are compatible with either an even slower aggradation or with a mostly autocyclic phase of channel shifting, the latter being more probable according to the observed strata geometries. This would then complete the picture of a phase of slow creation of accommodation space, in a transgressive phase driven by a slow sea level rise, followed, after a short forced regression, by a full highstand phase.

The base-level fall marking the transition between $S4_1$ and $S4_2$ determined the formation of the SB2 surface and of an inferred, likely interfluve soil (PS4f, Fig. 9B).

A higher amplitude base-level fall forced the transition between S4 and S5 synthems and the related SB4 surface, sculpted through the ongoing incision, was covered by a thin veneer of sediments derived from the dismantling of $S4_1$, including the PS4f soil (Fig. 9C). Such a thin sedimentary cover conceptually coincides with the Forced Regressive/Falling Stage Systems Tract (Hunt and Tucker, 1992; Plint and Nummedal, 2000) meaning that slope wasting accompanied the progressive sculpting of the SB4 surface, creating the shingled sedimentary wedges whose topmost and lowermost ends we observed at log 2 and log 1 respectively. The soil sediment features detected at these two locations account for different subaerial exposure in the time-transgressive development of the SB4 surface. Weak soil development detected on the deposits at log 2 points to relatively longer subaerial exposure of the older tract of this surface and covering deposits compared to the lack of pedogenic modification on the deposits at log 1. The latter accumulated from a mudflow, whose short exposure, in the final stage of SB4 development, did not allow any soil formation. The subsequent base-level rise (Fig. 9D), associated to marine flooding of the former coastal plain, determined the formation of the transgressive surface TS3, that, as a ravinement surface, reworked the falling stage deposits and their eventual pedogenic signature. The latter indicative of the maximum regressive surface expected to bound on top the

Forced Regressive/Falling Stage Systems Tract (Hunt and Tucker, 1992; Plint and Nummedal, 2000).

Despite the SB4-TS3 surface recording the higher-amplitude depositional shift in the composite sequential architecture of the succession, the intervening slope deposits don’t show evidence of significant soil formation as expected for the exposure of a major unconformable surface. This suggests that a relatively short time separated the base-level falling stage from the subsequent marine transgression, preventing soil processes differently from what predicted in the well-established sequence-stratigraphic models for non-marine/continental settings.

5. Conclusions

This study has provided an example of how palaeopedology and facies analysis may be integrated in deciphering the signals of cyclic sedimentation in continental settings. The results of this integration suggest that a robust picture may emerge when palaeosols and sediments are regarded as interrelated features providing information on the different processes acting in alluvial depositional systems. Specifically, in this case, channelized facies and palaeosols in the floodbasin facies of sub-unit $S4_1$ converge toward a palaeoenvironmental setting characterized by a markedly seasonal climate. This local condition determined a coherent scenario for sediment dispersal and weathering processes adding important detail to the general picture of a warm early Piacenzian to which these deposits are ascribed. The composite stacking of facies and palaeosols brings the discussion toward the modeling of the cyclic pattern of deposition driven by fluctuating base/sea-level. In a sequence-stratigraphic perspective the facies-palaeosol architecture of S4 synthem confirms in large part what described in well-established models of cyclothemic deposition in continental settings, but also allows to introduce some further refining. We suggest that changes in the frequency, thickness and degree of development of palaeosols within continental successions may be used to refine the definition of transgressive and highstand system tracts, with implications for palaeoenvironmental reconstruction. The pedo-sedimentary signature of a major sea-level fluctuation recorded in the transition between S4 and S5 synthem escapes from these models offering a different perspective on what may happen when a high-amplitude fall and rise of sea-level occur in a relatively short time. Under this condition the presented case suggests that a well-developed and drained palaeosol may not necessarily mark the maximum regressive surface shaped during the falling stage of sea-level as expected in the models.

Acknowledgements

References

Aldinucci, M., Benvenuti, M., Andreetta, A., Dominici, S., Foresi, L.M., Carnicelli, S. and Martini, I. 2019). Composite sequence stratigraphic patterns in alluvial to shallow-marine successions: Examples from the Piacenzian of the Valdelsa Basin (Central Italy). Sedimentary Geology 388, 99-113

Benvenuti, M., Degli Innocenti, D., 2001. The Pliocene deposits in the Central-Eastern Valdelsa Basin (Florence, Italy) revised through facies analysis and unconformity-bounded stratigraphic units. Rivista Italiana di Paleontologia e Stratigrafia 107, 265-286.

Benvenuti, M., Del Conte, S., 2013. Facies and sequence stratigraphic modeling of a Upper Pliocene–Lower Pleistocene fluvial succession (Valdelsa Basin, central Italy). Sedimentary Geology 294, 303–314.

Benvenuti, M., Bertini, A., Conti, C., Dominici, S., 2007. Integrated analyses of litho-and biofacies in a Pliocene cyclothemic, alluvial to shallow marine succession (Tuscany, Italy). Geobios 40, 143-158.

Benvenuti, M., Del Conte, S., Scarselli, N., Dominici, S., 2014. Hinterland basin development and infilling through tectonic and eustatic processes: latest Messinian-Gelasian Valdelsa Basin, Northern Apennines, Italy. Basin Research 26, 387–402.

Billi, P., Magi, M., Sagri, M., 1987. Coarse-Grained Low-Sinuosity River Deposits: Example from Plio-Pleistocene Valdarno Basin, Italy. In: Frank G. Ethridge, Romeo M. Flores, Michael D. Harvey (eds), Recent Developments in Fluvial Sedimentology, SEPM Spec. Pub, 39, 197-203

Birkeland, P.W., 1999. Soils and geomorphology. Oxford University Press, New York, 1999. No. of pages: 430

Bonini, M., Sani, F., Stucchi, E.G., Benvenuti, M., Menanno, G., Tanini, C., 2014. Late Miocene shortening of the Northern Apennines back–arc. Journal of Geodynamics 74, 1-31

Breecker, D.O., Sharp, Z.D., McFadden, L.D., 2009. Seasonal bias in the formation and stable isotopic composition of pedogenic carbonate in modern soils from central New Mexico, USA. Bulletin of the Geological Society of America 121, 630-640.

Capezzuoli, E., Foresi, L.M., Salvatorini, G., Sandrelli, F., 2005. New data on the Middle Pliocene sedimentation in the southern Valdelsa basin (Siena, Italy). Bollettino Società Geologica Italiana, Volume speciale 4, 95–103.

Carnicelli, S., Costantini, E.A.C., 2013. Time as a soil forming factor and age of Italian soils. In: E.A.C. Costantini, C. Dazzi (eds.): The Soils of Italy. Springer, Dordrecht Heidelberg New York London; pp. 93-104.

Cerling, T.E., 1984. The stable isotopic composition of modern soil carbonate and its relationship to climate. Earth and Planetary Science Letters 71, 229-240.

Cerling, T.E., Quade, J., 1993. Stable carbon and oxygen isotopes in soil carbonates. Climate Change in Continental Isotopic Records, Geophys. Monogr., 78, AGU, Washington, DC, pp. 217-231

Chakraborty, C., Bose, P.K., 1992. Ripple/dune to upper stage plane bed transition: some observations from the ancient record. Geological Journal 27, 349-359.

Cojan, I., Bialkowski, A., Gillot, T., Renard, M., 2013 Paleoenvironnement and paleoclimate reconstruction for the early to middle Miocene from stable isotopes in pedogenic carbonates (Digne-Valensole basin, southeastern France). Bulletin de la Société Géologique de France, 184, 583–599

Costantini, E.A.C., 2018. Paleosols and pedostratigraphy. Applied Soil Ecology 123, 597-600.

Del Conte, S., 2007. Dinamica deposizionale e fattori di controllo dei sistemi fluvio-deltizi e marino-costieri: il Bacino pliocenico della Valdelsa (Toscana Centrale, Italia). Unpublished Doctorate Thesis, University of Florence, Florence.

Di Celma, C., Pieruccini, P., Farabollini, P., 2015. Major controls on architecture, sequence stratigraphy and paleosols of middle Pleistocene continental sediments ("Qc Unit"), eastern central Italy. Quaternary Research 83, 565–581.

Dominici, S., Danise, S., Benvenuti, M., 2018. Pliocene stratigraphic paleobiology in Tuscany and the fossil record of marine megafauna. Earth-Science Reviews 176, 277-310.

Dowsett, H., Dolan, A., Rowley, D., Moucha, R., Forte, A.M., Mitrovica, J.X., Pound, M., Salzmann, U., Robinson, M., Chandler, M., Foley, K., Haywood, A., 2016. The PRISM4 (mid-Piacenzian) paleoenvironmental reconstruction. Climate of the Past 12, 1519–1538.

Driese, S.G., Ober, E.G., 2005. Paleopedologic and paleohydrologic records of precipitation seasonality from early Pennsylvanian "Underclay" palaeosols, U.S.A. Journal of Sedimentary Research, 75 (6), pp. 997-1010.

Fidolini, F., Andreetta, A., 2013. Integrating sedimentological and palaeopedological data for palaeoenvironmental reconstruction: Examples from the Plio-Pleistocene Upper Valdarno Basin (Northern Apennines, Italy). Italian Journal of Geosciences 132, 149-166.

Ghelardoni, R., Giannini, E., Nardi, R., 1968. Ricostruzione paleogeografica dei bacini neogenici e quaternari della bassa valle dell'Arno sulla base dei sondaggi e dei rilievi sismici. Memorie Società Geologica Italiana 7, 91-106.

Gile, L.H., Peterson, F.F., Grossman, B., 1966. Morphological and genetic sequences of carbonate accumulation in desert soils. Soil Sci. 101, 347–360.

Huth, T.E., Cerling, T.E., Marchetti, D.W., Bowling, D.R., Ellwein, A.L., Passey, B.H., 2019. Seasonal Bias in Soil Carbonate Formation and Its Implications for Interpreting High-Resolution Paleoarchives: Evidence From Southern Utah. Journal of Geophysical Research: Biogeosciences 124, 616-632.

Hunt, D., Tucker M.E., 1992. Stranded parasequences and the forced regressive wedge systems tract: deposition during base-level fall. Sedimentary Geology, 81, 1-9

IUSS-WRB, 2015. World reference base for soil resources. World Soil Resour. Rep. 103.

Kraus, M.J., 1999. Paleosols in clastic sedimentary rocks: their geologic applications. Earth Science Reviews 47, 41–70

Jopling, A.V., 1965. Hydraulic factors and shape of laminae. Journal of Sedimentary Petrology 35, 777–791.

Kim, S.T., O´Neil, J.R. (1997) Equilibrium and nonequilibrium oxygen isotope effects in synthetic carbonates. Geochim. Cosmochim. Acta. 61:3461-3475.

Machette, M.N., 1985. Calcic soils of the southwestern United States. In: Weide D.L., Faber M.L. (Eds.) - Soils and Quaternary Geology of the Southwestern United States. Geological Society of America. Special Paper 203, 1–21

Mack, G.H., Tabor, N.J., Zollinger, H.J., 2010. Palaeosols and sequence stratigraphy of the Lower Permian Abo Member, south-central New Mexico, USA. Sedimentology 57, 1566-1583.

Martini, I.P., Sagri, M., 1993. Tectono-sedimentary characteristics of the late Miocene-Quaternary extensional basins of the Northern Apennines, Italy. Earth-Science Reviews 34, 197-233.

McCarthy, P.J., Plint, A.G., 2013. A pedostratigraphic approach to nonmarine sequence Stratigraphy: a three-dimensional paleosol-landscape model from the cretaceous (Cenomanian) Dunvegan formation, Alberta and British Columbia, Canada. New Frontiers in Paleopedology and Terrestrial Paleoclimatology, SEPM Special Publication 104, 159–177.

McCarthy, P.J., Plint, A.G.,2014. Recognition of interfluve sequence boundaries: Integrating paleopedology and sequence stratigraphy. Geology 26, 387–390

McCrea, J.M. (1950) On the isotopic chemistry of carbonates and a paleotemperature scale. The Journal of Chem. Phys. 18: 849-857.

Mermut, A.R., Padmanabham, E., Eswaran, H., Dasog, Ghulappa., 1996. Pedogenesis. Vertisols and Technologies for their Management. Developments in Soil Science 24, 43-61.

Mitchum, R., M., Jr., Van Wagoner, J., C., 1990. High-frequency sequences and eustatic cycles in the Gulf of Mexico basin: Proceedings, Gulf Coast Section SEPM 11th Annual Research conference, 257–267.

Mutti, E., Davoli, G., Mora, S., Sgavetti, M., 1994. The eastern sector of the south-central folded Pyrenean foreland: Criteria for stratigraphic analysis and excursion notes. Second High Resolution Sequence Stratigraphy Conference. 83 pp. Università di Parma, Parma.

Pal, D.K., Wani, S.P., Sahrawat, K.L., 2012. Vertisols of tropical Indian environments: Pedology and edaphology. Geoderma 189-190, 28-49.

Plink-Björklund, P., 2015. Morphodynamics of rivers strongly affected by monsoon precipitation: Review of depositional style and forcing factors. Sedimentary Geology, 323, 110–147.

Plint, A. G., Nummedal, D., 2000. The falling stage systems tract: recognition and importance in sequence stratigraphic analysis. Geological Society, London, Special Publications, 172, 1-17.

Quade, J., Cerling, T.E., 2007. Carbonate stable isotopes: Non–lacustrine terrestrial studies, In SA Elias (Ed.) Encyclopedia of Quaternary Science, Elsevier, p. 339–351.

Raigemborn, M.S., Beilinson, E., 2020. Stratigraphic architecture and paleosols as basin correlation tools of the early Paleogene infill in central–south Patagonia, Golfo San Jorge Basin, Argentinean Patagonia. Journal of South American Earth Sciences, 99

Retallack, G.J., 2001. Soils of the Past: An Introduction to Paleopedology: Blackwell Science Publishers, Oxford. 404 p.

Schoeneberger, P.J., Wysocki, D.A., Benham, E.C., Soil Survey Staff, 2012. Field Book for Describing and Sampling Soils, Version 3.0. Natural Resources Conservation Service, National Soil Survey Center, Lincoln, NE.

Shanley, K.W., McCabe, P.J. 1994. Perspectives on the sequence stratigraphy of continental strata. AAPG Bulletin 78, 544–568.

Sheldon, N.D., 2005. Do red beds indicate paleoclimatic conditions?: A Permian case study. Palaeogeography, Palaeoclimatology, Palaeoecology 228, 305-319.

Tabor N.J., Myers, T.S., 2015. Paleosols as Indicators of Paleoenvironment and Paleoclimate. Ann. Rev. Earth Planet. Sci. 43, 333–61

Vepraskas, M.J., 1999. Redoximorphic features for identifying aquic conditions: North Carolina Agricultural Research. Service Tech. Bull., 301, 229. North Carolina State University, Raleigh.

Wright, V.P. 1992. Paleosols: Their Recognition and Interpretation. Princeton Series in Geology and Paleontology, 340 pp

Wright, V.P., Marriott, S.B., 1993. The sequence stratigraphy of fluvial depositional systems: the role of floodplain sediment storage. Sedimentary Geology 86, 203–210.

Figure captions

Fig. 1: conceptual scheme of fluvial deposition and soil development during a cycle of relative base-level variation (after Wright and Marriott, 1993)

Fig. 2: A) location of the study area; B) detail of the geological map of the study sites with location of the logged sections; C) oblique aerial view from Google Earth™ looking north, annotated for the location of the logged sections; D) simplified stratigraphic log of the S4-S6 synthems in the study area (Aldinucci et al., 2019 for details)

Fig. 3: Correlation panel of the logged sections (Fig. 2B-C for location; after Aldinucci et al., 2019) showing the stratigraphic architecture of the upper portion of S4 synthem with palaeosols profiles, the transition to S5 and its facies stack. Different ranking of key-bounding surfaces outlines the composite sequential architecture of the studied succession. Codes: lst/LST: low stand systems tract; tst/TST: transgressive systems tract; hst/HST: highstand systems tract; MFS: maximum flooding surface; CS: condensed section; FST: falling-stage systems tract

Fig. 4: Panorama of the section of log 3 (Figs. 2 and 3 for location) with annotation of facies, palaeosols and EDSs.

Fig. 5: The S4-S5 transition at log 1 showing detail of the deposits included between the SB4 and TS3 surfaces

Fig. 6: The S4-S5 transition at log 2 (A) showing the deposits bracketed between the SB4 and TS3 surfaces; B) detailed view of the graded beds with carbonate nodules lag; C) close-up view of the sharp TS3 surface separating greyish inner shelf fossiliferous mudstone from mottled silty sandstones. Rod in B) and C) is 1-meter long.

Fig. 7: Palaeosols and sampled carbonate nodules: A) Calcic Regosol (PS4a); B) Vertisol (PS4c); C) Calcic Vertisol (PS4d); D) detail of log 1 showing a highly developed Calcic horizon (PS4f); E) carbonate nodules collected in the soil sediments at log 1; F) detail of oximorphic feature in a well-developed Calcic horizon at log 2 (PS4f); G) carbonate nodules collected from the soil sediments at log 2: left to right, top to bottom beds; top nodules have oximorphic iron-manganese coatings; the shape of nodules is typical of pedogenic carbonates (Schoeneberger et al., 2012).

Fig 8 Cross-diagram of carbon and oxygen isotope composition of carbonate nodules collected at the S4-S5 transition

Fig. 9: Sequence-stratigraphic model for the development of the Piacenzian succession in the study area. A) vertical aggradation of EDS in the highstand systems tract of CDS1: palaeosols hint to increasing development in time; B) base level fall marking the transition between $S4_1$ and $S4_2$: the well-drained soil PS4f developed on the interfluve of an incised valley; C) an higher-magnitude progressive base-level fall following the aggradation of $S4_2$ brought to the development of SB4 surface draped by successive wedges of sediments along the slope bearing a fully reworked PS4f; D) the successive rise of base/sea-level determined the infill of a wide palaeovalley with the S5 shallow marine deposits. Wave erosion due to rising sea-level produced the TS3 ravinement surface

Table 1: Synthetic description of the facies types in the studied portion of the succession (after Aldinucci et al., 2019)

Table 2: Palaeosol description, classification (IUSS-WRB Working Group, 2015) and position within the stratigraphic sequence.

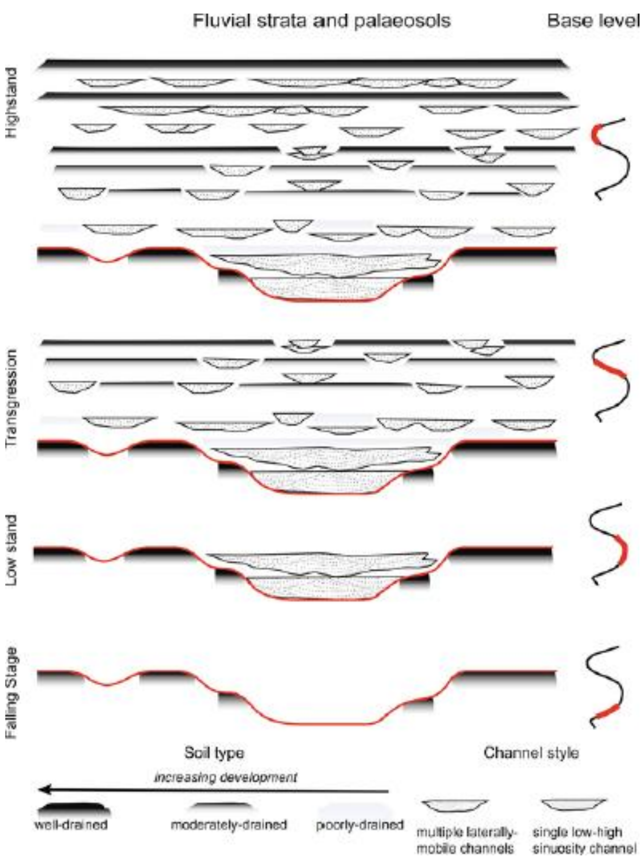

Fig. 1

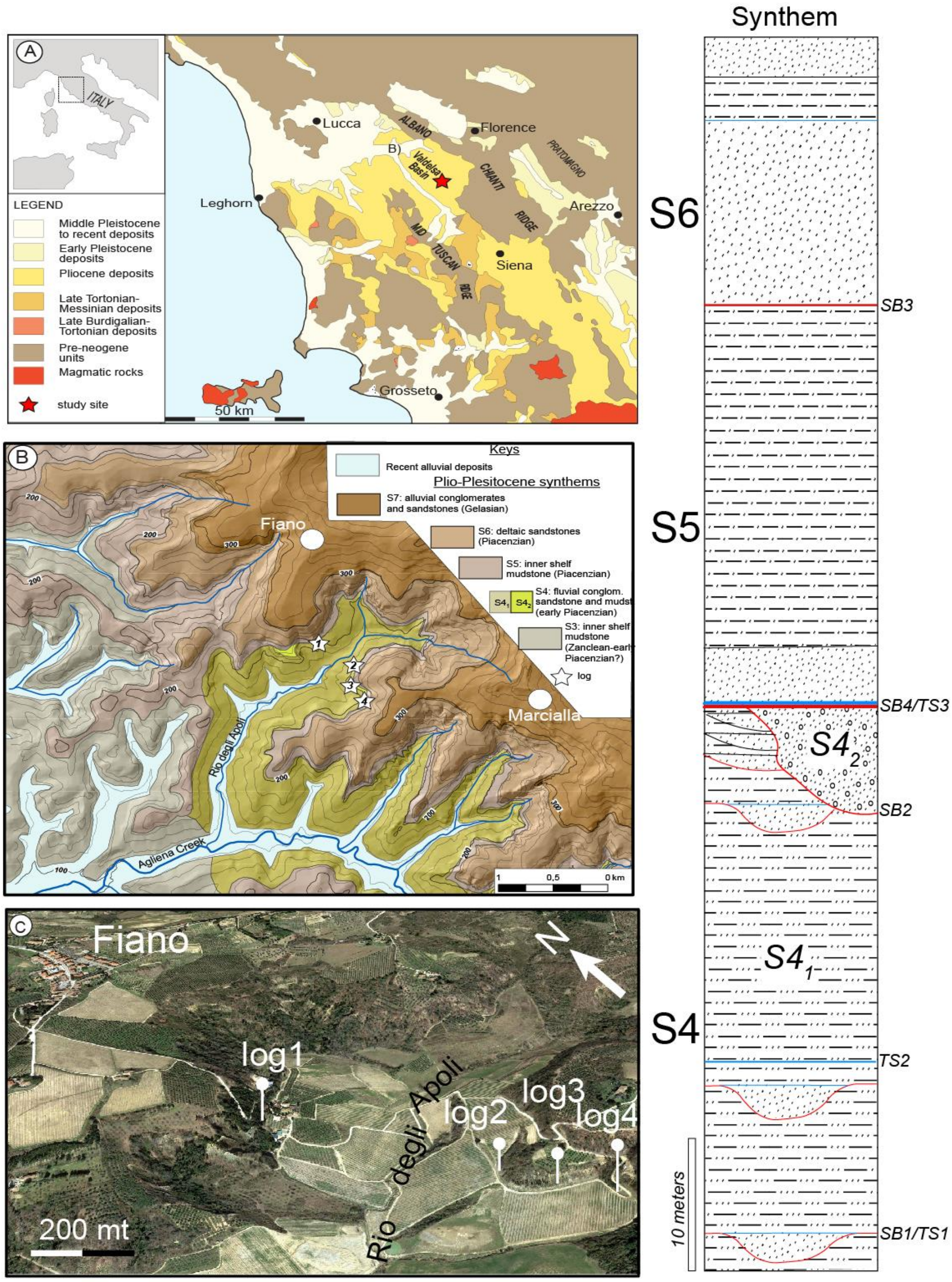

A
ITALY
LEGEND
Middle Pleistocene to recent deposits
Early Pleistocene deposits
Pliocene deposits
Late Tortonian-Messinian deposits
Late Burdigalian-Tortonian deposits
Pre-neogene units
Magmatic rocks
study site
Lucca
Florence
Leghorn
Arezzo
Siena
Grosseto
ALBANO
CHIANTI
RIDGE
PRATOMAGNO
MID TUSCAN RIDGE
Valdelsa Basin
B)
50 km
B
Keys
Recent alluvial deposits
Plio-Plesitocene synthems
S7: alluvial conglomerates and sandstones (Gelasian)
S6: deltaic sandstones (Piacenzian)
S5: inner shelf mudstone (Piacenzian)
S4: fluvial conglom. sandstone and mudst (early Piacenzian)
S3: inner shelf mudstone (Zanclean-early Piacenzian?)
log
Fiano
Marcialla
Rio degli Apoli
Agliena Creek
1 0,5 0 km
C
Fiano
N
log1
log2
log3
log4
Rio degli Apoli
200 mt
Synthem
S6
S5
S4
SB3
SB4/TS3
S4₂
SB2
S4₁
TS2
SB1/TS1
10 meters

Fig. 2

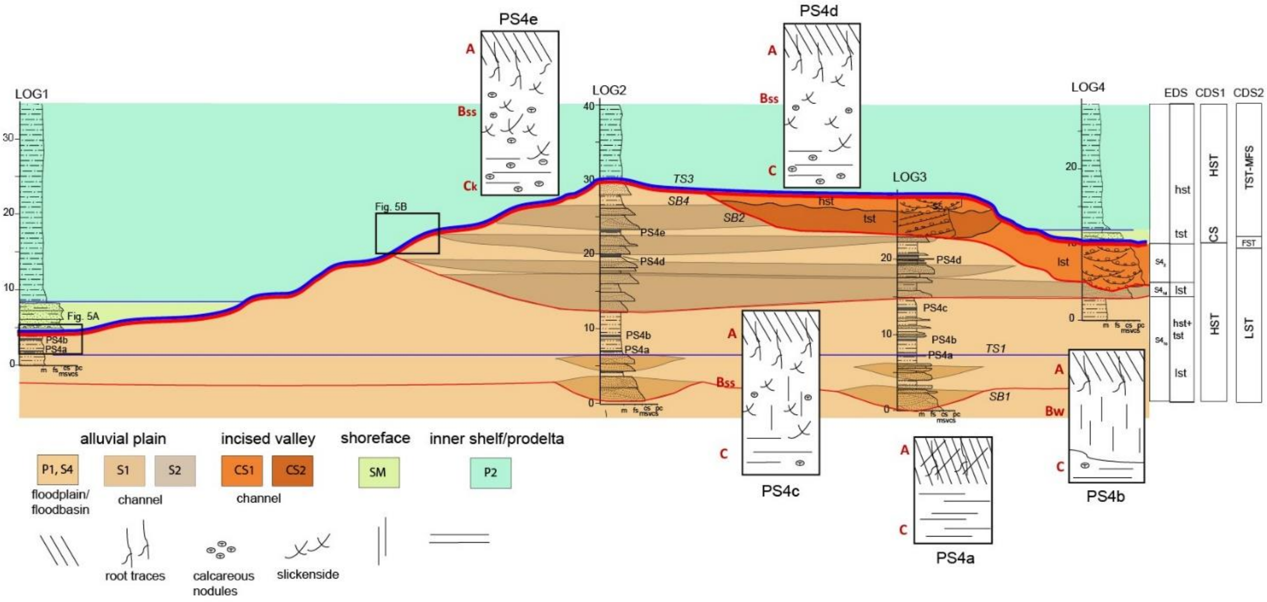
LOG1
LOG2
LOG3
LOG4
PS4e
PS4d
PS4c
PS4b
PS4a
Fig. 5A
Fig. 5B
TS3
SB4
SB2
TS1
SB1
hst
tst
lst
EDS
CDS1
CDS2
HST
CS
TST-MFS
FST
LST
alluvial plain
incised valley
shoreface
inner shelf/prodelta
P1, S4
S1
S2
CS1
CS2
SM
P2
floodplain/
floodbasin
channel
channel
root traces
calcareous
nodules
slickenside

Fig. 3

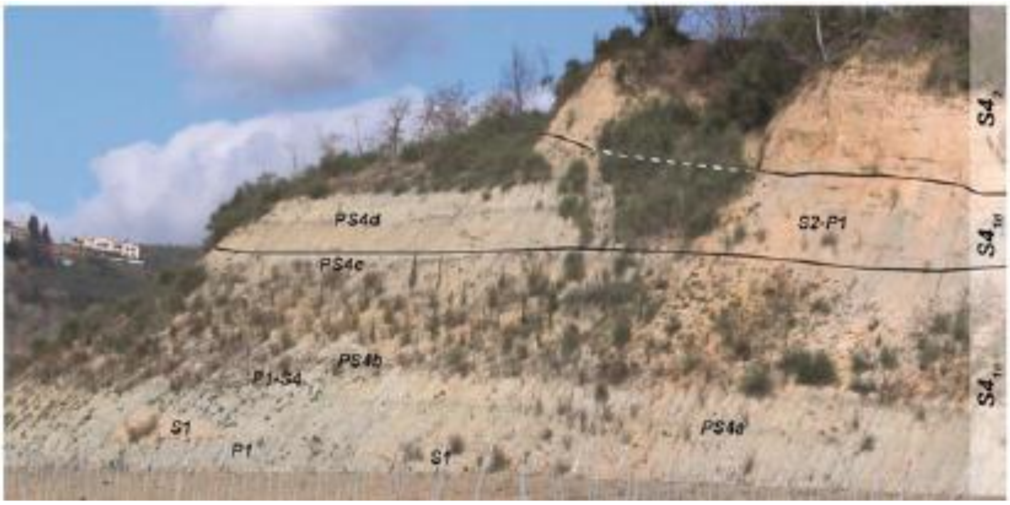
PS4d
PS4c
PS4b
P1-S4
S1
P1
S1
PS4a
S2-P1

Fig. 4

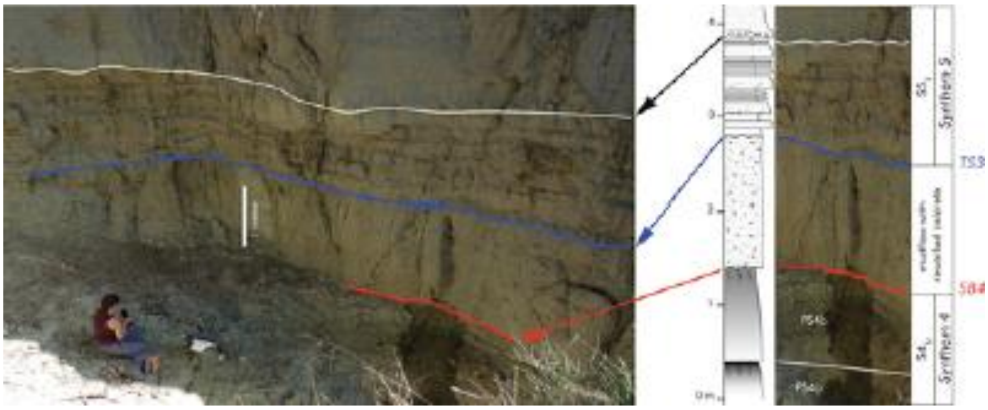

Fig. 5

Fig. 6

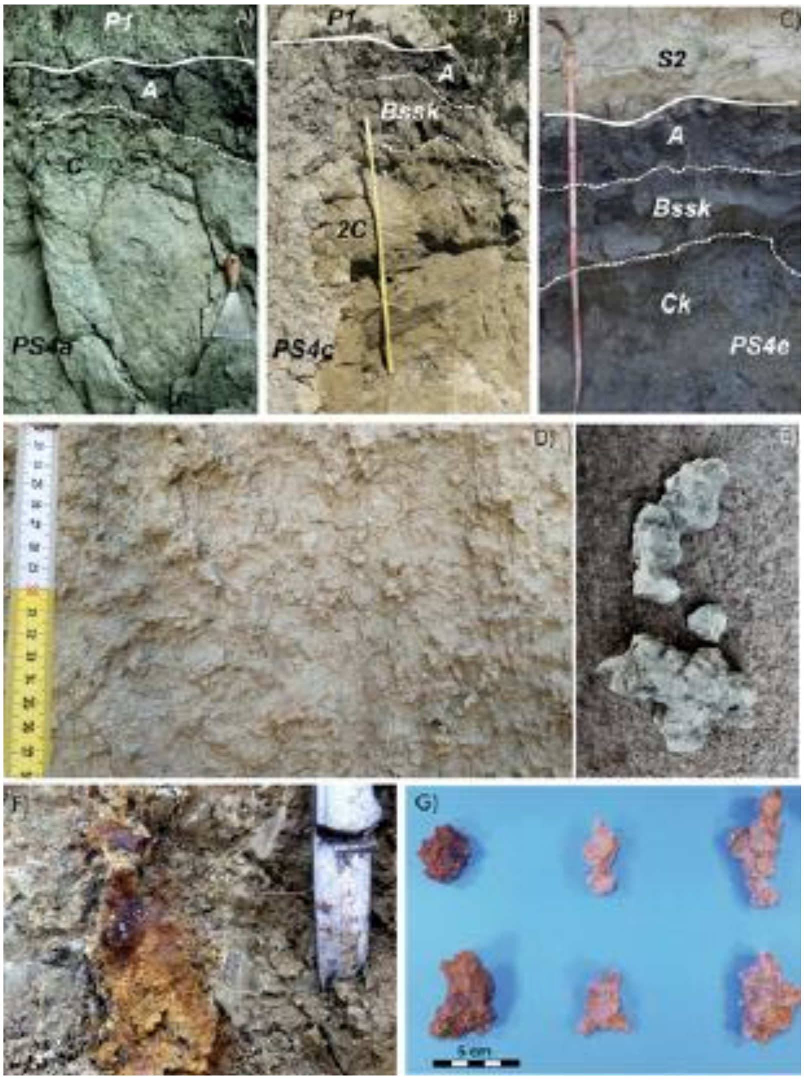
P1
A
C
PS4a
P1
A
Bssk
2C
PS4c
S2
A
Bssk
Ck
PS4e
D)
E)
F)
G)
5 cm

Fig. 7

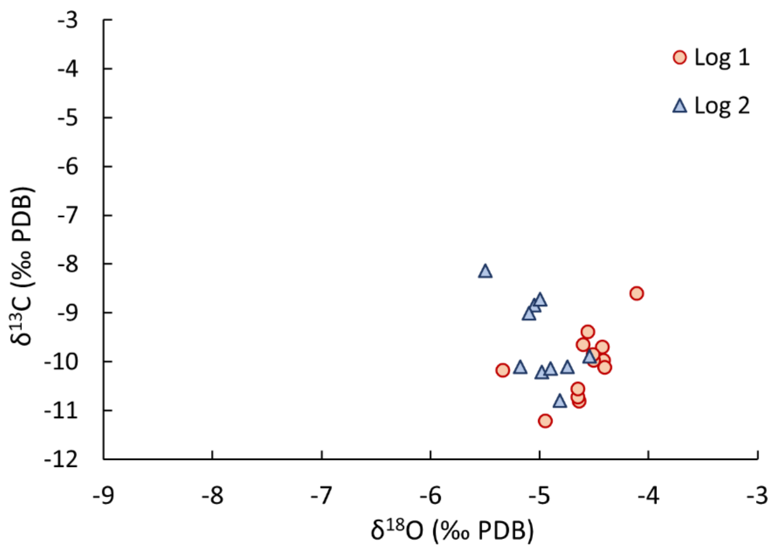
Log 1
Log 2
δ13C (‰ PDB)
δ18O (‰ PDB)
-3
-4
-5
-6
-7
-8
-9
-10
-11
-12
-9
-8
-7
-6
-5
-4
-3

Fig. 8

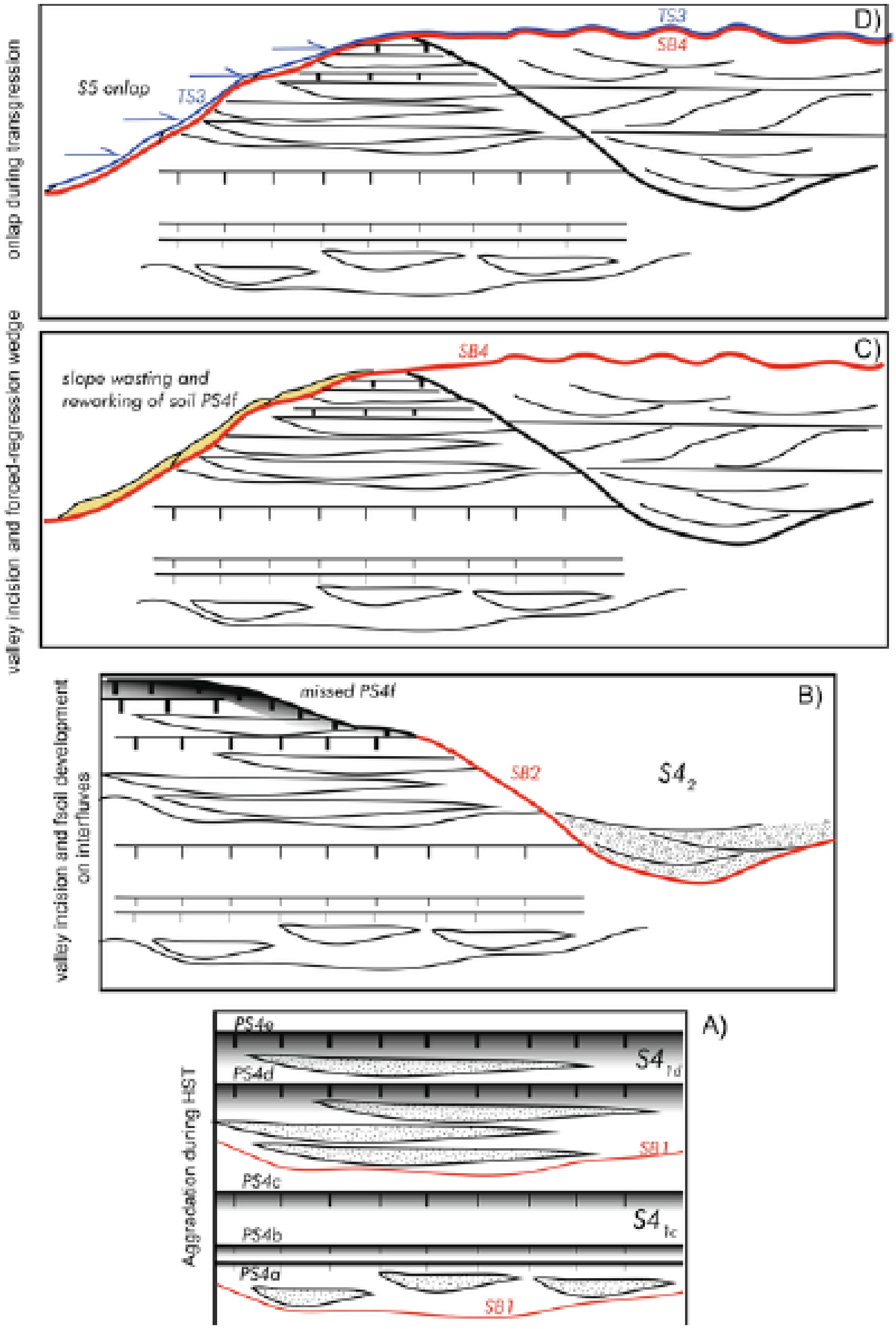
D)
TS3
SB4
S5 onlap
TS3
onlap during transgression
C)
SB4
slope wasting and
reworking of soil PS4f
valley incision and forced-regression wedge
B)
missed PS4f
SB2
$S4_2$
valley incision and fsoil development
on interfluves
A)
PS4e
$S4_{1d}$
PS4d
SB1
PS4c
$S4_{1c}$
PS4b
PS4a
SB1
Aggradation during HST

Fig. 9

S4: yellowish medium-fine sandstone in meter-scale sheet -like bedsets with a convex top. Bedsets include decimetre-thick plane beds with a massive, graded or horizontal laminated structure. Rare occurrence of climbing ripples.

PS: alternation of yellowish-greyish fine-medium sandstone and greyish massive-graded sandy mudstone. Sandstones in decimetre-thick plane beds are massive bearing marine mollusc shell debris or disarticulated shells. Occasional symmetric ripples draped by mudstone. Occurrence of shell debris

P2: greyish massive sandy mudstone. Diffuse and/or concentrated marine gastropods and bivalve shells commonly in life position

P1: light to dark grey massive mudstone with common mottling, carbonate nodules, darker horizons (see paleosol description). Occurrence of carbonized vegetal remains, rare shells of terrestrial molluscs, root traces

CS2: alternation of brownish pebble-cobble conglomerate and sandstone in decimetre thick planar inclined beds dipping to WNW. Locally embedded decimetre-thick trough-cross lenses of pebbly sandstone indicating paleocurrent to SSW.

CS1: alternation of brownish pebble-cobble conglomerate and sandstone in meter-scale amalgamated through-cross beds. The framework is clast-supported with well -rounded clasts and local abundant interstitial sandy matrix. Clast imbrication and bed geometry indicate paleocurrent to SSW

S2: yellowish coarse-medium sandstone in meter-scale sheet-like bedsets with a concave base. Amalgamated beds are characterized by trough-cross or low-angle planar cross lamination. Pebble lags may occur at the base of single beds. Rare fragments of carbonized vegetal matter

S1: yellowish coarse-medium sandstone in meter-scale lenticular bedsets with a concave base. Beds are graded or cross-laminated. Dip of laminae indicates paleocurrent to SSW. Centimetre-thick mudstone are occasionally interbedded with sandstone

Table 2

Palaeosol	Horizon	Depth (cm)	Matrix colour	Structure	Redox colours	Carbonates	Other	Soil classification	Position
PS4a	A	0-15/25	2.5Y 4/1	ABKm3			rare slickensides	Calcaric Fluvisol weak Vertic and Calcic features	P1 facies, EDS S41c, lower part, above TS1 surface
	2Cr	15/25-(60)	2.5Y 6/1	S		coatings on cracks			
PS4b	A	0-10/15						Haplic Cambisol weak Vertic and Calcic features	P1 facies, EDS S41c, lower-middle part
	Bw	10/15-25/30					rare slickensides		
	2Cr	25/30-(50)				rare pseudomycelia			
PS4c	A	0-5/11	7.5YR 2.5/1	PRf3				Calcic Vertisol	P1 facies, EDS S41c, upper part
	Bssk	5/11-35	7.5YR 4/2	WEGm2		common soft masses	intersecting slickensides		
	2BC	35-95	10YR 6/3	PRc2					
PS4d	A	0-10/15	5Y 4/1	ABKm2	7.5YR 4/4		rusty channels	Vertic Calcisol	P1 facies, EDS S41d, middle part
	Bss	10/15-45/60	5Y 5/2	PRc2	7.5YR 5/8	rare soft masses	rusty channels and slickensides		
	2Ck	45/60-110+	5/10GY	S	10YR 4/6	common cemented masses (Ø=2 cm)	rusty channels (gleyic pattern)		
PS4e	A	0-17/25	2.5Y 4/1	PRf3		small soft masses	pressure faces	Calcic Vertisol	P1 facies, EDS S41d, upper part
	Bssk	17/25-35/42	2.5Y 4/1	WEGc3	7.5YR 4/6	common cemented masses (Ø=2 cm)	intersecting slickensides		
	2Ck	35/42-70+	2.5Y 6/3	S		abundant cemented masses (Ø=2 cm)	(gleyic pattern)		
PS4f						abundant nodules (Ø=1-4 cm)	post-reworking Gleyic features	highly developed Stage II Calcic horizon	Eroded by SB4/TS3